JOC The Journal of Organic Chemistry

Article

pubs.acs.org/joc

Alkylammonium Cation Complexation into the Narrow Cavity of Dihomooxacalix[4]arene Macrocycle

Carmine Gaeta,*[,†] Carmen Talotta,[†] Francesco Farina,[†] Filipa A. Teixeira,[‡] Paula M. Marcos,*[,‡,∥] José R. Ascenso,[§] and Placido Neri*[,†]

[†]Dipartimento di Chimica e Biologia, Università di Salerno, Via Ponte don Melillo, I-84084 Fisciano (Salerno), Italy

[‡]Centro de Ciências Moleculares e Materiais, Faculdade de Ciências da Universidade de Lisboa, Edifício C8, 1749-016 Lisboa, Portugal

[∥]Faculdade de Farmácia da Universidade de Lisboa, Av. Prof. Gama Pinto, 1649-003 Lisboa, Portugal

[§]Instituto Superior Técnico, Complexo I, Av. Rovisco Pais, 1049-001 Lisboa, Portugal

Supporting Information

ABSTRACT: How big should a calixarene macrocycle be for *endo*-cavity complexation to occur or to allow *through-the-annulus* threading? To answer these questions, a complete study on the complexation of primary and secondary (di)alkylammonium cations by 18-membered *p-tert*-butyldihomooxacalix[4]arene macroring has been performed in the presence of the "superweak" TFPB counterion. Thus, it was found that this macrocycle is currently the smallest calixarene able to host linear and branched alkylammonium guests inside its aromatic cavity. Molecular mechanics calculations revealed that this recognition event is mainly driven by a H-bonding interaction between the guest ammonium group and the host CH_2OCH_2 bridge. The *endo*-cavity complexation of chiral *s*-$BuNH_3^+$ guest results in an asymmetric complex in the NMR time scale. The chirality transfer from guest to host is likely due to a restricted guest motion inside the tight cavity. The complexation study with secondary di-*n*-alkylammonium·TFPB salts revealed that the 18-membered dihomooxacalix[4]arene macroring cannot give the *through-the-annulus* threading with them because of its small dimension. However, the macrocycle is able to complex such ions, which can only be accommodated in an hook-like conformation characterized by two unfavorable gauche interactions around the $CH_2-NH_2^+$ bonds. The strain generated by this unfavorable folding is very likely compensated by stronger H-bonds and more favorable CH/π interactions between guest and host.

INTRODUCTION

Molecular recognition is a fundamental process within biological systems. In the last decades, several artificial hosts have been synthesized that are able to mimic the natural ones and that provide applications for developing technologies such as sensing devices. In this regard, particular attention has been devoted to the study of *endo*-cavity complexation by macrocycles such as calix[*n*]arenes,[1] cyclodextrins,[2] crown ethers,[3] and cucurbiturils.[4] In contrast, the *endo*-complexation ability of dihomooxacalix[4]arene macrocycle,[5] a calix[4]arene analogue in which one CH_2 bridge is replaced by one CH_2OCH_2 group, still remains largely unstudied.[5b]

Recently,[6] we have obtained the first examples of *endo*-cavity complexation of large calixarene macrocycles with alkylammonium organic cations[7] by exploiting the inducing effect of the weakly coordinating Tetrakis[3,5-bis(triFluoromethyl)Phenyl]-Borate ($TFPB^-$) "superweak anion".[8] Our method works very well with simple calixarene ethers and no extensive or sophisticated chemical modifications of the parent macrocycles are required. Thus, following this "superweak anion" approach, we have reported the first example of *endo*-cavity complexation of primary alkylammonium ions with large calix[6]arene derivative **1b** (Chart 1).[6a] This approach was successively extended to conformationally blocked doubly bridged calix[7]-arene[9] derivative **2** in which *endo*-complexation of alkylammonium cations occurs within the 24-membered subring.[10] It is noteworthy that no hint of *endo*-complexation of alkylammonium guests was observed with both calixarene hosts **1** and **2** in the presence of more tightly coordinating anions such as Cl^-, PF_6^-, and $B(Ph)_4^-$.[6,10] Very recently, the effectiveness of our "superweak anion" approach has been corroborated by Chiu and co-workers,[11] who have shown that TFPB anion is able to enhance the binding affinity between [24]-crown-8 hosts and dibenzylammonium guests.

Further examples of primary alkylammonium *endo*-complexation by calixarenes regard the 20-membered calix[5]arene ring, which is able to host linear guests,[7a,b,f,g,l,12] whereas to the best of our knowledge, no examples of such complexation by 16-membered calix[4]arene ring have been so far reported. Therefore, how big a calixarene macrocycle should be for such *endo*-cavity complexation to occur is a basic question in

Received: September 13, 2012
Published: October 12, 2012

Chart 1

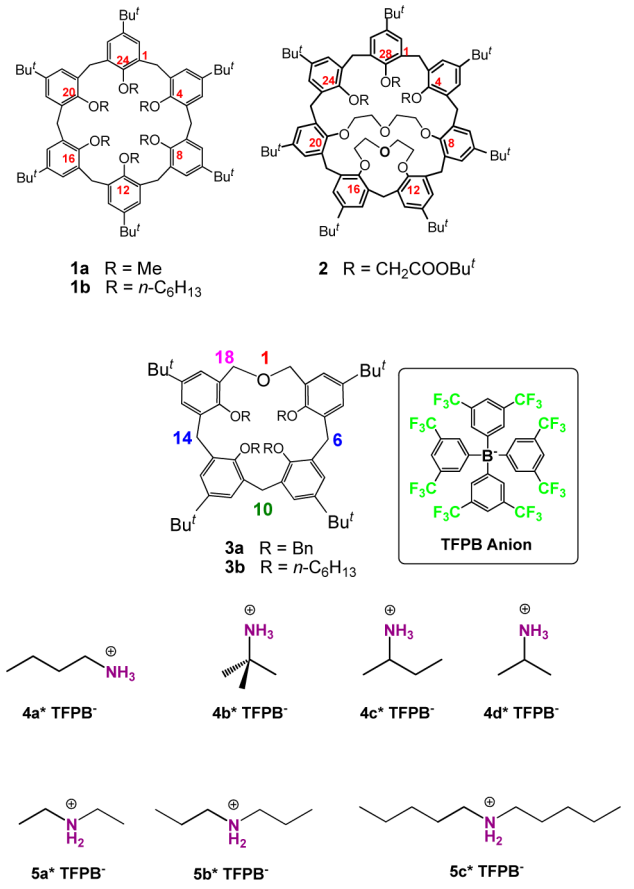

molecular recognition with calixarene hosts. A second strictly related question concerns the minimum dimension of a calixarene macrocycle which would allow the *through-the-annulus* threading with secondary dialkylammonium ions. In fact, such threading has been so far observed for 24-membered calix[6]arenes[6] **1a**,**b** and for 20-membered calix[5]arenes,[13] whereas no data have been reported for the smaller analogues. At this regard is useful to know that in the crown ether series the lower limit for dialkylammonium threading has been currently set to the 21-membered ring of [21]crown-7 macrocycle,[14a] which was consequently used to prepare the smallest known rotaxane.[14b]

An ideal probe to answer both questions is the 18-membered dihomooxacalix[4]arene macrocycle **3** (Chart 1),[5] which possesses an intermediate size between those of calix[4]- and -[5]arenes (16- and 20-membered, respectively). Thus, prompted by these considerations and considering the known beneficial influence of conformational preorganization on the host abilities,[6a] we decided to study the molecular recognition properties of conformationally blocked cone-shaped *p-tert*-butyldihomooxacalix[4]arene derivatives **3a**,**b** toward alkylammonium and di-*n*-alkylammonium ions **4a**,**d** and **5a**−**c** (Chart 1), and we report here the results of these studies.

RESULTS AND DISCUSSION

Binding Ability of Dihomooxacalix[4]arene Derivative 3a toward Primary, Linear *n*-Butylammonium Guest 4a. ^{1}H NMR experiments, at room temperature, showed interesting recognition properties for *p-tert*-butyldihomooxacalix[4]arene derivative **3a** toward alkylammonium TFPB$^-$ salt **4a** (Chart 1). In particular, the addition of the TFPB salt of *n*-butylammonium cation **4a** to a $CDCl_3$ solution of **3a**, at 298 K, gave significant changes in its ^{1}H NMR spectrum (Figure 1).

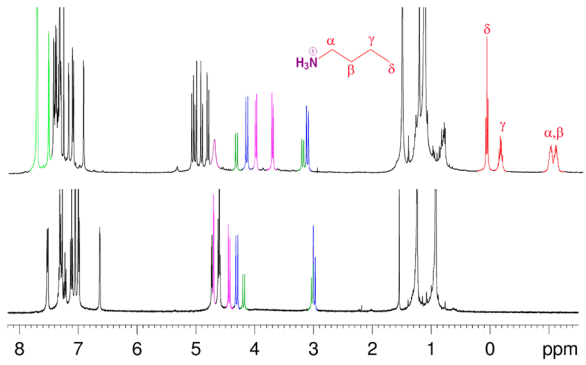

Figure 1. ^{1}H NMR spectra ($CDCl_3$, 400 MHz, 298 K) of: (bottom) **3a** and (top) an equimolar solution (3 mM) of **3a** and *n*-butylammonium **4a**·TFPB$^-$. The coloring of the signals corresponds to that used in the structure drawings reported above and in Chart 1.

The most evident ones were the appearance of a new set of slowly exchanging signals due to the *n*-BuNH_3^+⊂**3a** complex formation and the presence of *n*-butyl resonances in the upfield negative region of the spectrum (Figure 1). This is a clear indication that the linear *n*-butylammonium cation **4a** gave an *endo*-cavity complexation with the alkyl chain shielded by the aromatic rings. Complex formation was also confirmed by an ESI(+) mass spectrum which gave as the base peak a value of 1112.7 *m*/*z* corresponding to supramolecular ion *n*-BuNH_3^+⊂**3a**. A COSY-45 spectrum[15] allowed a complete confident assignment of all *n*-BuNH_3^+ resonances. Thus, NH_3^+ group at 4.72 ppm correlates with α protons at −0.96 ppm, which in turn show a coupling with β methylene group at −1.01 ppm, which presents a cross-peak with γ protons at −0.10 ppm, finally coupled with δ methyl at 0.13 ppm. In a 2D ROESY spectrum,[15] the *n*-BuNH_3^+⊂**3a** complex gives rise to ROE correlations among the shielded β, γ, and δ signals at −1.01, −0.10, and 0.13 ppm, respectively, and the aromatic protons of the host in *ortho* to the *tert*-butyl groups at 6.94 (d, J = 2.4 Hz), 7.20 (d, J = 2.1 Hz), 7.35 (d, J = 2.4 Hz), and 7.46 ppm (d, J = 2.1 Hz).

In this way, it was clear that the *n*-butyl protons that experience the highest complexation induced shift (CIS) are those at the α position which undergo an upfield shift of 3.84 ppm, while the protons at the β, γ, and δ positions experience a CIS of 2.87, 1.58, and 1.05 ppm, respectively. Interestingly, the upfield shift experienced by the α protons of guest **4a** (3.84 ppm) is very similar to that previously observed for its analogous *endo* complexation with a calix[5]arene host (3.86 ppm),[12a] whereas it is significantly higher with respect to that obtained with larger calix[6,7]arene macrocycles ($\Delta\delta$ = 2.89 and 2.62 ppm, respectively).[6,10] Very likely, the *n*-butylammonium guest **4a** is more tightly wrapped into the narrow cavity of dihomooxacalix[4]arene **3a** with respect to the larger calix[6,7]arene cavities. In fact, this binding mode was confirmed by the lowest AMBER energy[16] structure of *n*-BuNH_3^+⊂**3a** complex (Figure 2, left), where it is possible to measure an average distance of 3.85 Å between α protons of guest **4a** and the centroid of the aromatic rings of **3a**, a value significantly lower than that observed with larger calix[6,7]arene hosts (4.76 and 4.49 Å, respectively).[6a,10]

dx.doi.org/10.1021/jo3019945 | J. Org. Chem. 2012, 77, 10285−10293

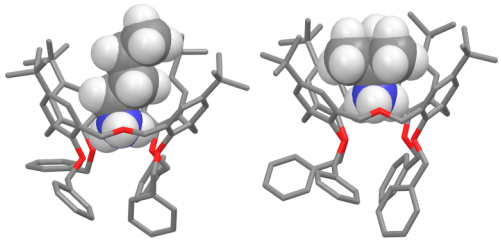

Figure 2. Lowest AMBER energy structures of *n*-$BuNH_3^+$⊂**3a** (left) and *t*-$BuNH_3^+$⊂**3a** (right) complexes.

An additional interesting feature observable in the lowest energy structure of *n*-$BuNH_3^+$⊂**3a** complex (Figure 2, left) is a slight tilting of butylammonium guest, with respect to the central axis of the host cavity, to allow H-bond formation with both *O*-atoms of the ethereal bridge and of the lower rim of dihomooxa macrocycle. The first H-bond pulls out the butylammonium guest **4a** from the host cavity as demonstrated by the 1.48 Å distance of *N*-atom of **4a** with the mean plane of the lower rim oxygens, which is significantly higher than that observed for an analogous calix[6]arene complex (0.76 Å).[6a,10] Thus, molecular mechanics calculations revealed that the *endo*-complexation of **4a** into the aromatic cavity of **3a** is mainly driven by the H-bonding interaction between the ammonium group and the more basic ethereal *O*-bridge. Therefore, this H-bond is fundamental for the stability of the complex.

An apparent association constant of 5.5 ± 0.4 × 10^6 M^{-1} (Table 1) was determined for *n*-$BuNH_3^+$⊂**3a** complex by means of an ^{1}H NMR competition experiment with guest **4d** in $CDCl_3$ (400 MHz, 298 K) (see below).[17a] Interestingly, this value was significantly higher than that observed for the complexation of **4a** with a calix[7]arene host (5.2 × 10^3 M^{-1}),[10] likely because of the higher preorganization of the smaller dihomooxacalix[4]arene macroring. It is noteworthy that no hint of complexation of *n*-$BuNH_3^+$ guest was observed for **3a**, in $CDCl_3$ at 298 K, in the presence of counterions such as Cl^-, PF_6^-, and $B(Ph)_4^-$, probably due to their stronger ion-pairing tendency with respect to the more hydrophobic and weakly coordinating $TFPB^-$ anion. As expected, a similar effect was also observed with competing H-bonding-acceptor solvents, since we found that the addition of 320 equiv of DMSO led to a complete decomplexation of the *n*-butylammonium guest of *n*-$BuNH_3^+$⊂**3a** complex (10 mM in $CDCl_3$).

As a primary conclusion from the above results, we can now answer the first question raised above: within the calixarene family of macrocycles, alkylammonium *endo*-complexation can occur down to the 18-membered macroring of dihomooxacalix[4]arenes.

Binding Abilities of Dihomooxacalix[4]arene 3a toward Branched Alkylammonium Guests 4b–d. At this point, it is interesting to study the binding abilities of dihomooxacalix[4]arene **3a** toward branched alkylammonium guests and to compare them with those of larger calix[5]arene derivatives. In fact, Pappalardo and co-workers[18] have reported a remarkable selectivity of calix[5]arenes toward linear alkylammonium ions, whereas no interaction could be detected with bulky *t*-$BuNH_3^+$ ion **4b**, even in the presence of a large excess of it. At a first glance, it could be expected that the smaller 18-membered ring of **3a** may give rise to an even higher selectivity for linear alkylammonium ions than the 20-membered calix[5]arene macrocycle.

Surprisingly, we found that the addition of solid *t*-$BuNH_3^+$·$TFPB^-$ salt to a $CDCl_3$ solution of **3a** caused again dramatic changes in its ^{1}H NMR spectrum (400 MHz, 298 K, Figure S11, Supporting Information), with the appearance of a singlet in the upfield negative region (at −0.57 ppm) attributable to the *t*-Bu group of **4b** hosted inside the aromatic cavity of **3a**. Complex formation was also confirmed by ESI(+) MS and 2D ROESY NMR.

In particular, the ESI(+) mass spectrum gave the base peak at 1112.7 *m*/*z* corresponding to the supramolecular ion *t*-$BuNH_3^+$⊂**3a**. In the 2D ROESY spectrum ($CDCl_3$, 400 MHz, 298 K), dipolar correlations were observed between the shielded *t*-Bu signal at −0.57 ppm and the four calixarene ArH resonances at 6.89, 7.12, 7.29, and 7.38 ppm (Figure 3). A

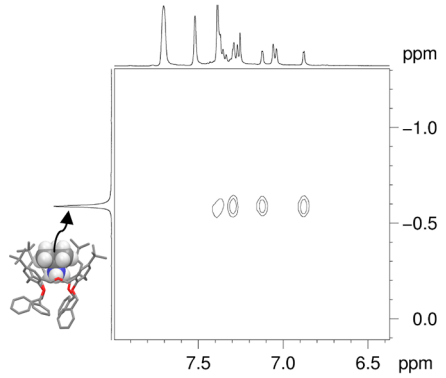

Figure 3. Section of the ROESY spectrum of *t*-$BuNH_3^+$⊂**3a** complex ($CDCl_3$, 400 MHz, 298 K).

quantitative ^{1}H NMR experiment[17b] led to an apparent association constant (Table 1) for slowly exchanging the *t*-$BuNH_3^+$⊂**3a** complex of 3.1 ± 0.3 × 10^4 M^{-1}, a value significantly lower than that observed for linear *n*-$BuNH_3^+$⊂**3a** (5.5 × 10^6 M^{-1}, selectivity ratio = K_{assoc}(*n*-$BuNH_3^+$)/K_{assoc}(*t*-$BuNH_3^+$) = 177).

Very likely, with respect to branched *t*-$BuNH_3^+$ guest **4b**, the linear *n*-$BuNH_3^+$ guest **4a** is able to penetrate more deeply into the cavity of **3a**, for steric reasons, positioning its ammonium group more closer to the lower rim oxygen atoms of **3a**. This difference was confirmed by comparing the lowest AMBER energy structure of *t*-$BuNH_3^+$⊂**3a** and *n*-$BuNH_3^+$⊂**3a** complexes (Figure 2, right and left, respectively), obtained with the MacroModel-9.0 program.[16] In particular, is possible to observe the *tert*-butyl group inside the cavity of **3a** with the nitrogen atom sitting at a distance of 2.2 Å above the mean plane of

Table 1. Association Constants (K_{assoc}, M^{-1}) of Alkylammonium 4a–d Complexes with Dihomooxacalix[4]arene Host 3a Determined by ^{1}H NMR Spectroscopy (400 MHz, $CDCl_3$, 298 K)

	n-$BuNH_3^+$·$TFPB^-$	*t*-$BuNH_3^+$·$TFPB^-$	*s*-$BuNH_3^+$·$TFPB^-$	*i*-$PrNH_3^+$·$TFPB^-$
3a	5.5 ± 0.4 × 10^{6a}	3.1 ± 0.3 × 10^{4b}	3.6 ± 0.2 × 10^{4b}	7.6 ± 0.5 × 10^{4b}

[a]Determined by ^{1}H NMR competition experiment treating 1 equiv of **3a** in $CDCl_3$ with a mixture of **4a** and **4d** TFPB salts (1 equiv each). [b]Determined by quantitative ^{1}H NMR analysis of its 1:1 titration mixture in $CDCl_3$ using 1,1,2,2-tetrachloroethane as internal standard.

dx.doi.org/10.1021/jo3019945 | J. Org. Chem. 2012, 77, 10285–10293

calixarene *O*-atoms at the lower rim of **3a**, a value significantly higher with respect to that observed (1.5 Å) for *endo*-cavity complexation of *n*-$BuNH_3^+$ guest with **3a** (Figure 2, left). Consequently, the ammonium group of **4b** is hydrogen-bonded only to the bridged oxygen atom of **3a** (Figure 2, right), indicating that this H-bond is the fundamental driving force for complex formation. This conclusion was confirmed by inspection of the 2D ROESY spectrum that revealed the presence of diagnostic cross-peaks between shielded *t*-Bu signal at −0.57 ppm and $ArCH_2OCH_2Ar$ bridge protons at 4.16 and 3.91 ppm. The same argument of balance between penetration depth and steric encumbrance can be used to explain the different behavior of **3a** with respect to calix[5]arenes. In fact, the lower penetration in *t*-$BuNH_3^+$⊂**3a** still allows the formation of a stabilizing H-bond with only a low steric demand, whereas a similar H-bonding in calix[5]arenes would require a deeper penetration with a too high steric repulsion. It is interesting to point out that, as above for **4a**, no hint of interaction was detected between *t*-$BuNH_3^+$ guests **4b** and **3a** in the presence of counterions such as Cl^-, PF_6^-, and $B(Ph)_4^-$, in $CDCl_3$ at 298 K, confirming the effectiveness of our "superweak anion" approach.

The extension of ^1H NMR complexation studies ($CDCl_3$, 400 MHz, 298 K) to racemic *sec*-butylammonium ion **4c** revealed again spectral changes (Figure 4) similar to those

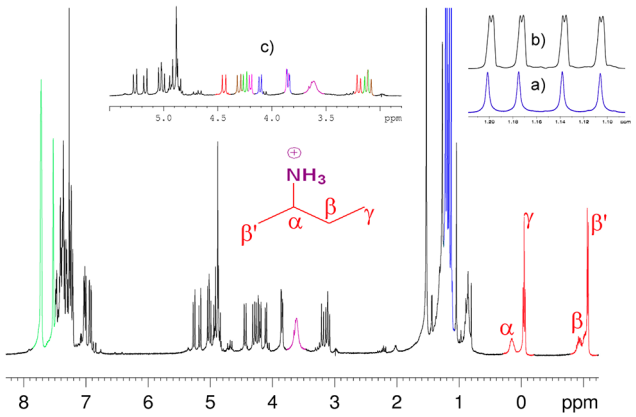

Figure 4. ^1H NMR spectrum ($CDCl_3$, 400 MHz, 298 K) of an equimolar solution (3 mM) of **3a** and *s*-butylammonium **4c**·$TFPB^-$. Inset: *t*-Bu region of the ^1H NMR spectrum ($CDCl_3$, 400 MHz, 298 K) of **4c**⊂**3a** complex in the presence (b) and in the absence (a) of Pirkle's reagent. Inset (c): ^2J-coupled methylene protons are highlighted by identical colors.

discussed above, with the appearance of upfield resonances pertinent to guest *s*-Bu group inside the aromatic cavity of **3a**. A base peak at 1112.7 *m/z* in the ESI(+) mass spectrum confirmed the formation of *s*-$BuNH_3^+$⊂**3a** complex. A COSY−45 spectrum[15] ($CDCl_3$, 400 MHz, 298 K) allowed a complete assignment of all *s*-$BuNH_3^+$ resonances evidencing an higher CIS for both *β′* methyl [−1.06 ppm (*d*, *J* = 8.0 Hz)] and diastereotopic *β* methylene group (−0.94 and −0.96 ppm) (Figure 4). Surprisingly, a closer inspection of the COSY−45 spectrum[15] revealed the presence of 5 AX systems (see, Figure 4c) at 4.46/3.21, 4.31/3.12, 4.22/3.86, 4.21/3.15 and 4.11/3.85 ppm for the five $ArCH_2$− bridging groups, which are consistent with an asymmetric structure of *s*-$BuNH_3^+$⊂**3a** complex. In accordance, the calix *t*-Bu groups give rise to four distinct singlets at 1.12, 1.16, 1.19, and 1.22 ppm (see Figure 4a), confirming the chiral nature of the complex. The racemic nature of *s*-$BuNH_3^+$⊂**3a** complex was evidenced by the doubling of *t*-Bu resonances in its ^1H NMR spectrum ($CDCl_3$, 400 MHz, 298 K) upon addition of Pirkle's reagent [(*S*)-(+)-(9-anthryl)-2,2,2-trifluoroethanol] (see Figure 4b). Thus, the inclusion of the chiral *s*-$BuNH_3^+$ guest into the achiral *p-tert*-butyldihomooxacalix[4]arene host **3a** results in a chiral *s*-$BuNH_3^+$⊂**3a** supramolecule. In particular, the loss of symmetry of **3a** must be due to a restricted motion of the branched *s*-$BuNH_3^+$ guest into the narrow oxacalix cavity of **3a** (see Figure 5). This was confirmed by VT ^1H NMR studies of

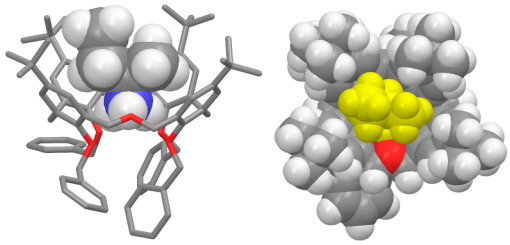

Figure 5. Lowest energy structure of *s*-$BuNH_3^+$⊂**3a** complex found by Monte Carlo conformational search (10000 steps, MacroModel V. 9.0, AMBER force field). (Left) side view. (Right) top view (in yellow *s*-$BuNH_3^+$ guest).

s-$BuNH_3^+$⊂**3a** complex (in $C_2D_2Cl_4$) that evidenced symmetrical spectra for host **3a** only at temperatures above 353 K, leading to an estimated energy barrier of 19.2 kcal/mol.

The exact positioning of the Me and Et *α*-branches of **4c** inside the cavity of **3a** was predicted by the lowest energy structure of *s*-$BuNH_3^+$⊂**3a** (Figure 5) and was confirmed by the relevant ROE correlations between those groups and ArH (see Figure S4c, Supporting Information[15]), *t*-Bu, and CH_2OCH_2 signals. In particular, all *s*-$BuNH_3^+$ protons gave diagnostic ROE correlations with the CH_2OCH_2 bridge (see Figure S4d, Supporting Information[15]) and with *t*-Bu groups adjacent to CH_2OCH_2 bridge (see Figure S4e, Supporting Information[15]). Very likely, this particular positioning allows formation of stronger H-bonds with a higher number of stabilizing CH−*π* interactions.

It is worth pointing out that this transfer of chirality[19] from chiral guest to achiral host is rather uncommon on the NMR time scale. In fact, in the analogous complexation *s*-$BuNH_3^+$ ion by larger calix[6,7]arene hosts no such transfer was observed, leaving the host symmetrical on the NMR time scale.[10] The apparent association constant for slowly exchanging *s*-$BuNH_3^+$⊂**3a** complex (Table 1) was determined by ^1H NMR ($CDCl_3$, 400 MHz, 298 K) signal integration[17b] to give a value of $3.6 \pm 0.2 \times 10^4$ M^{-1}. Interestingly, once again, this value was significantly higher than that observed for the complexation of guest **4c** with a larger calix[7]arene host (6.2×10^2 M^{-1}).[10]

Interesting results were also obtained for the complexation of secondary *i*-$PrNH_3^+$ ion **4d**. In fact, the ^1H NMR spectrum (400 MHz, 298 K, Figure S10, Supporting Information) of a 1:1 mixture of TFPB salt of **4d** and **3a** in $CDCl_3$ showed a doublet at −1.00 ppm (*J* = 6.8 Hz) and a broad signal at 0.28 ppm for *β*-CH_3 and *α*-CH protons, respectively, of the *endo*-cavity-included isopropyl group of **4d**. ^1H NMR quantitative analysis (400 MHz, 298 K) of a 1:1 mixture of **3a** and **4d** in $CDCl_3$ revealed an apparent association constant for *i*-$PrNH_3^+$⊂**3a** complex of $7.6 \pm 0.5 \times 10^4$ M^{-1} (Table 1),[17b] a value slightly higher than that observed for the complexation of *s*-$BuNH_3^+$ (3.6×10^4 M^{-1}), which is only slightly more bulky.

dx.doi.org/10.1021/jo3019945 | J. Org. Chem. 2012, 77, 10285−10293

Binding Abilities of Dihomooxacalix[4]arene Derivative 3a,b toward Secondary Dialkylammonium Guests 5a−c. In order to answer the second question concerning the smaller threadable calixarene macrocycle we studied the binding ability of **3a** toward diethylammonium guest **5a**, which can be considered as one of the less encumbering axles.

In contrast to the above results obtained with primary alkylammonium guests **4a−d**, the addition of diethylammonium guest **5a** (Chart 1) to a $CDCl_3$ solution of **3a** (400 MHz, 298 K) caused shifts of the host signals due to a fast complexation equilibrium on the NMR time scale (Figure 6).

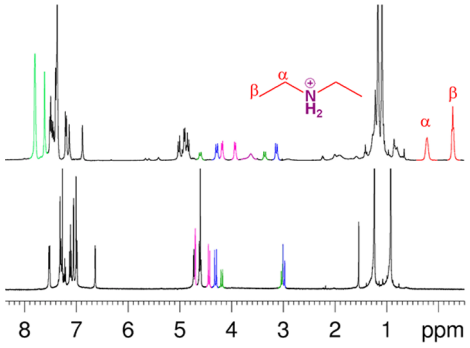

Figure 6. (Bottom) ^{1}H NMR spectrum (400 MHz, $CDCl_3$, 298 K) of **3a**. (Top) ^{1}H NMR spectrum (400 MHz, $CDCl_3$, 298 K) of an equimolar mixture of **3a** (3 mM) and diethylammonium **5a**·TFPB$^-$. The coloring of the signals corresponds to that used in the structure drawings reported above and in Chart 1.

Table 2. Association Constants (K_{assoc}, M^{-1}) of Di-*n*-alkylammonium Complexes 5a−c with Dihomooxacalix[4]arene Hosts 3a and 3b Determined by ^{1}H NMR Titration Experiments (400 MHz, $CDCl_3$, 298 K)

	5a·TFPB$^-$	5b·TFPB$^-$	5c·TFPB$^-$
3a	$1.3 \pm 0.2 \times 10^5$		
3b	$6.0 \pm 0.2 \times 10^5$	$3.4 \pm 0.4 \times 10^3$	$4.5 \pm 0.4 \times 10^3$

Thus, a 1:1 complexation stoichiometry was determined by Job's plot ($CDCl_3$, 400 MHz, 298 K),[17a] while an apparent association constant of $1.3 \pm 0.2 \times 10^5$ M^{-1} (Table 2) for the **5a⊂3a** complex was determined by NMR titration experiments ($CDCl_3$, 400 MHz, 298 K) and nonlinear curve-fitting of the host chemical shift changes.[17a] Interestingly, a COSY−45 spectrum of an equimolar solution of **3a** and **5a** (400 MHz, $CDCl_3$, 298 K) evidenced the presence of a single set of shielded ethyl signals of guest **5a**. In fact, a scalar *J*-coupling was observed between the NH_2^+ ammonium protons (3.59 ppm) and their linked α protons at 0.23 ppm, which in turn showed a coupling with β protons at −0.26 ppm. In this way, it was clear that α and β protons of diethylammonium guest experience a CIS of 2.73 and 1.52 ppm, respectively, under the above conditions. These data were indicative of the inclusion of the diethylammonium guest **5a** within an aromatic cavity of the host **3a** and can be explained by two different binding modes, namely (a) the *endo*-complexation inside the homooxa cavity and (b) the *exo*-complexation at the lower rim oxygens with a concomitant shielding by the appended benzyl groups.

Both binding modes were studied by molecular mechanics calculations (Monte Carlo conformational search, 10000 steps, MacroModel V. 9.0, AMBER force field, $CHCl_3$ solvent, GB/SA model) (Figure 7), which evidenced stabilizing H-bonds in both instances. However, the *endo*-cavity complex (Figure 7, left) was found more stable by 3 kcal/mol with respect to the *exo*-cavity complex (Figure 7, right).

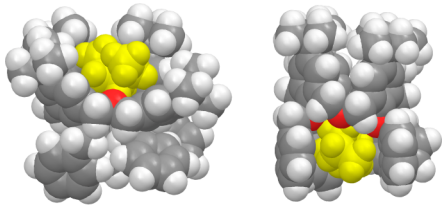

Figure 7. Lowest energy structure of *endo*- (left) and *exo*-cavity (right) **5a⊂3a** complex obtained by Monte Carlo conformational search (10000 steps, MacroModel V. 9.0, AMBER force field). Yellow: **5a** guest.

In order to obtain a definitive proof of such *endo*-cavity complexation, we decided to study the complexation of diethylammonium guest **5a** with dihomooxacalix[4]arene host **3b** bearing *n*-hexyl aliphatic chains at the lower rim. In this way, shielded guest resonances are ruled out in the case of *exo*-cavity complexation and would only be compatible with an *endo*-complexation. Therefore, tetrahexyloxydihomooxacalix[4]arene **3b** was synthesized by a standard NaH-promoted alkylation of the parent macrocycle, and its ^{1}H NMR spectrum (Figure 8b) ($CDCl_3$, 400 MHz, 298 K) in the presence of an equimolar amount of **5a** was acquired.

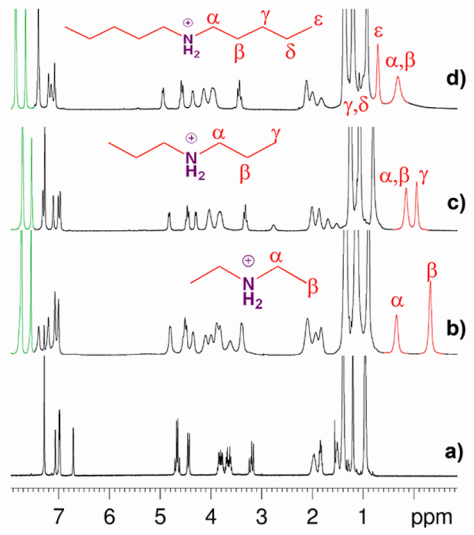

Figure 8. ^{1}H NMR spectra ($CDCl_3$, 400 MHz, 298 K) of (a) **3b**, (b) an equimolar solution (3 mm) of **3b** and **5a**, (c) an equimolar solution (3 mm) of **3b** and **5b**, (d) an equimolar solution (3 mm) of **3b** and **5c**.

As shown in Figure 8b, it revealed the presence of shielded α and β protons of diethylammonium guest **5a** at 0.40 and −0.26 ppm, respectively. A COSY−45 spectrum (Figure 9) of the same solution confirmed this assignment as evidenced by the consecutive scalar *J*-coupling between NH_2^+ (3.62 ppm), α (0.40 ppm), and β protons (−0.26 ppm). Thus, α and β protons of **5a** experienced a CIS of 2.56 and 1.52 ppm, respectively, upon complexation with **3b**, which is very similar to that observed by complexation with **3a** ($\Delta\delta$ = 2.73 and 1.52 ppm, respectively).

As stated above, the shielding experienced by the α and β protons of diethylammonium guest **5a** is only compatible with

dx.doi.org/10.1021/jo3019945 | J. Org. Chem. 2012, 77, 10285−10293

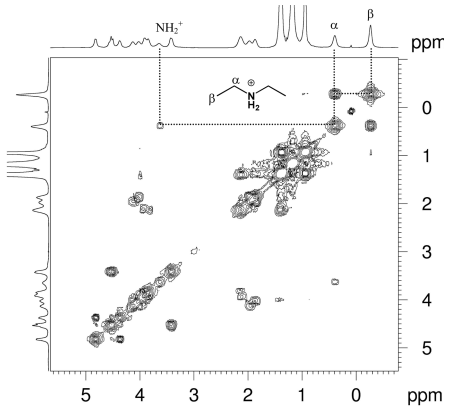

Figure 9. Portion of the COSY-45 spectrum ($CDCl_3$, 400 MHz, 298 K) of an equimolar solution (3 mM) of **3b** and diethylammonium **5a**·TFPB$^-$.

an *endo*-cavity **5a**⊂**3b** complex formation, which was further confirmed by the relevant dipolar correlations observed in a ROESY spectrum (400 MHz, $CDCl_3$, 298 K) among the shielded α and β protons of **5a** and the upper rim ArH protons of host **3b**. In the lowest AMBER energy structure of the complex **5a**⊂**3b** (Figure 10a–c), the diethylammonium guest is found sandwiched inside the aromatic cavity of **3b** with its *N*-atom involved in hydrogen bonding with both *O*-atoms of the CH_2OCH_2 bridge and hexyloxy pendant groups. Interestingly, it can also be evidenced (Figure 10a,b) that the diethylammonium guest cannot be accommodated in the more stable, fully extended anti conformation inside the aromatic cavity of dihomooxacalix[4]arene host **3b**, but it must adopt a hook-like shape, characterized by two unfavorable gauche conformations around the CH_2–NH_2^+ bonds (Figure 10c). This situation resembles those observed by Rebek in the encapsulation of long alkanes in a coiled form inside a self-assembled capsule.[20] In analogy to those complexes, in our case, the energy loss due to the folding of the diethylammonium guest to a less stable more compact form is counterbalanced by stronger H-bonds and more favorable CH/π interactions between the guest and host (Figure 10b).

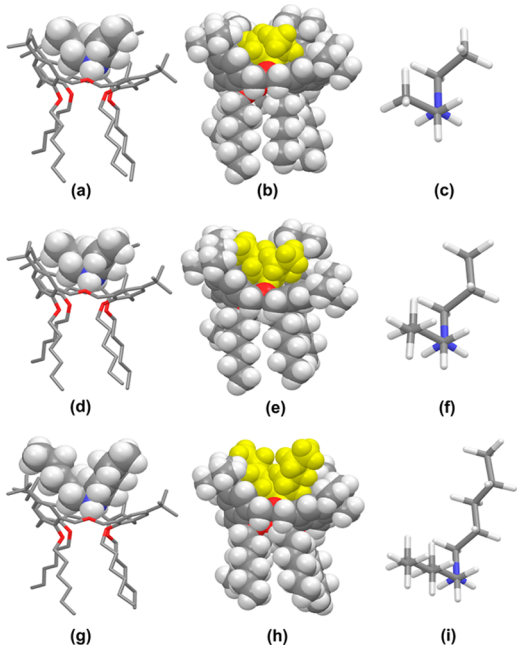

Figure 10. Lowest energy structure of **5a**⊂**3b** (a–c), **5b**⊂**3b** (d–f), and **5c**⊂**3b** (g–i) complexes found by Monte Carlo conformational search (10000 steps, MacroModel V. 9.0, AMBER force field). (a, d, g) Side view of the complexes. (b, e, h) CPK model of the complexes (in yellow di-*n*-alkylammonium guest **5a**–**c**). (c, f, i) Hook-like conformation adopted by dialkylammonium guests **5a**, **5b**, and **5c**, respectively, inside the cavity of **3b**.

Analogously to **3a**, the inclusion complex between **3b** and **5a** is fast exchanging on the NMR time scale ($CDCl_3$, 400 MHz, 298 K); consequently, its 1:1 stoichiometry was determined by Job's plot ($CDCl_3$, 400 MHz, 298 K).[17a] In addition, an apparent association constant for the **5a**⊂**3b** complex of 6.0 ± 0.2 × 10^5 M^{-1} was determined by NMR titration experiments ($CDCl_3$, 400 MHz, 298 K) (Table 2) and nonlinear curve-fitting.[17a]

In a similar way, the addition of longer di-*n*-alkylammonium guests, such as di-*n*-propyl- **5b** and di-*n*-pentylammonium **5c** (Chart 1), to a solution of **3b** in $CDCl_3$ again caused signal shifts due to a fast complexation equilibrium (400 MHz, 298 K) (Figure 11). A COSY-45 spectrum of an equimolar solution of **3b** and **5b** (400 MHz, $CDCl_3$, 298 K) evidenced the presence of a single set of shielded propyl signals of **5b**.[15] In fact, a scalar *J*-coupling was observed between the α protons at 0.27 ppm and the β protons at 0.29 ppm, which present a cross-peak with γ protons at 0.08 ppm (see the ^{1}H NMR spectrum in Figure 8c). Interestingly, the CIS experienced by α protons of **5b** is very similar to that observed for α protons of guest **5a** ($\Delta\delta$ = 2.89 and 2.65 ppm, respectively, Figure 8b,c), indicating a comparable *endo*-cavity complexation.

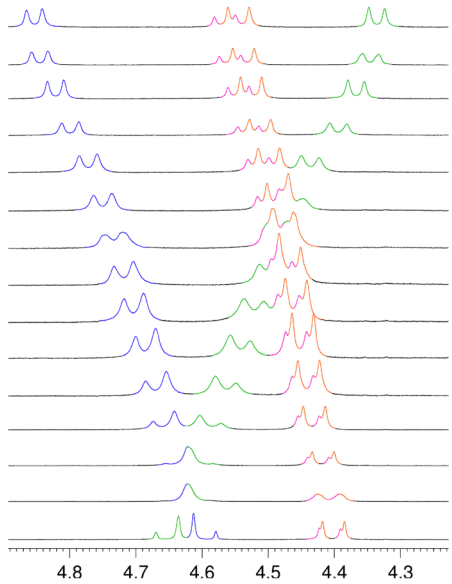

Figure 11. Titration of **3b** with di-*n*-propylammonium **5b**·TFPB$^-$. Region of the ^{1}H NMR spectrum ($CDCl_3$, 400 MHz, 298 K) of **3b** after addition of (from bottom to top) 0.0, 0.1, 0.2, 0.3, 0.4, 0.5, 0.6, 0.7, 0.8, 0.9, 1.0, 1.2, 1.4, and 1.6 equiv of di-*n*-propylammonium **5b**·TFPB$^-$.

This binding mode was confirmed by the lowest Amber energy structure of the complex **5b**⊂**3b** (Figure 10d–f) where the di-*n*-propylammonium guest is inside the aromatic cavity of **3b** with its *N*-atom involved in a significant hydrogen-bonding interaction with bridge *O*-atom. Analogously to diethylammo-

dx.doi.org/10.1021/jo3019945 | J. Org. Chem. 2012, 77, 10285–10293

nium guest **5a**, molecular mechanics calculations (Figure 10f) evidenced that a folding of the di-*n*-propylammonium guest **5b** must occur during the complexation process.[20] Again, the dipropylammonium guest adopts a bent shape characterized by two gauche conformations around the $CH_2-NH_2^+$ bonds (Figure 10f).

The complexation of the longer di-*n*-pentylammonium guest **5c** by host **3b** was studied in a similar manner. Again, the 1D ^1H NMR (Figure 8d) spectrum ($CDCl_3$, 400 MHz, 298 K) evidenced the presence of a single set of shielded *n*-pentyl signals,[15] with ε, δ, γ, β, and α protons resonating at 0.72, 1.01, 1.01, 0.38, and 0.38 ppm, respectively. A similar CIS (2.89 ppm) was observed for the α protons of guest **5c**, and a similar binding mode was confirmed by the lowest energy structure of the complex **5c⊂3b** (Figure 10g–i). Also in this case a folded conformation (Figure 10i) of di-*n*-pentylammonium guest was necessary to permit its accommodation inside the narrow cavity of **3b**.

Analogously to **5a⊂3b**, a 1:1 stoichiometry for **5b⊂3b** and **5c⊂3b** complexes was determined by Job's plot, while an apparent association constant of $3.4 \pm 0.4 \times 10^3$ and $4.5 \pm 0.4 \times 10^3$ M^{-1}, respectively, was determined by NMR titration experiments ($CDCl_3$, 400 MHz, 298 K) (Table 2).[17a] Interestingly, these values were significantly lower than those observed for guest **5a** ($6.0 \pm 0.2 \times 10^5$ M^{-1}), likely because the cavity of the 18-membered dihomooxacalix[4]arene **3b** is a better size match for the smallest diethylammonium guest **5a**.

From the above results, it is clear that the *through-the-annulus* threading with secondary dialkylammonium ions cannot occur with the 18-membered macroring of dihomooxacalix[4]arenes, which is too small to be threaded by such linear axles. The possibility of a threading with a very slow kinetic, as observed by Pappalardo and co-workers for a calix[5]arene derivative,[13] was ruled out by long equilibration experiments at 333 K (>72 h) between hosts **3a,b** and secondary dialkylammonium guests **5a–c**, which gave no hint of threading. This conclusion was corroborated by molecular mechanics calculations which gave optimized threaded structures with energy higher by 11–13 kcal/mol with respect to the corresponding lowest energy *endo*-cavity complex.

CONCLUSION

In conclusion, we have shown that the 18-membered dihomooxacalix[4]arene macroring is currently the smallest macrocycle belonging to the calixarene family able to host linear and branched primary alkylammonium guests inside its aromatic cavity in the presence of the "superweak" TFPB anion. This slow-exchanging *endo*-cavity complexation is mainly driven by the H-bonding interaction between the guest ammonium group and the CH_2OCH_2 bridge *O*-atom of the host. Differently with respect to the larger 20-membered *p-tert*-butylcalix[5]arene homologue, interaction with the 18-membered dihomooxacalix[4]arene macroring was also detected for isomeric branched tertiary *t*-$BuNH_3^+$ cation. Interestingly, *endo*-cavity complexation of chiral *s*-$BuNH_3^+$ guest by *p-tert*-butyldihomooxacalix[4]arene **3a** results in a *s*-$BuNH_3^+$⊂**3a** complex, which is asymmetric on the NMR time scale. The chirality transfer from the guest to the host is very likely favored by the restricted motion of the guest inside the narrow cavity of **3a**.

Finally, we have found that the 18-membered dihomooxacalix[4]arene macroring cannot give the *through-the-annulus* threading with secondary dialkylammonium ions because of its small dimension. On the contrary, such dialkylammonium guests give rise to a fast-exchanging *endo*-cavity complexation thanks to the above-mentioned H-bonding between the guest NH_2^+ group and the bridge *O*-atom of the host. The unexpected accommodation of the rather large di-*n*-alkylammonium cations inside the narrow cavity of 18-membered dihomooxacalix[4]arene ring requires their folding in a hook-like conformation characterized by two unfavorable gauche[20] interactions around the $CH_2-NH_2^+$ bonds. The corresponding stability loss is very likely counterbalanced by stronger H-bonds and more favorable guest/host CH/π interactions.

The information obtained in this work can be considered an interesting contribution to a deeper understanding of supramolecular interactions in host/guest systems and could be particularly useful in the design of new receptors for organic cations.

EXPERIMENTAL SECTION

General Experimental Methods. ESI(+)-MS measurements were performed on a triple quadrupole mass spectrometer equipped with electrospray ion source, using $CHCl_3$ as solvent. All chemicals were reagent grade and were used without further purification. Anhydrous solvents were used as purchased from supplier. When necessary, compounds were dried in vacuo over $CaCl_2$. Reaction temperatures were measured externally. Derivative **3a**,[5d] *n*-$BuNH_3^+$ tetrakis[3,5-bis(trifluoromethyl)phenyl]borate **4a**,[6a] *t*-$BuNH_3^+$ tetrakis-[3,5-bis(trifluoromethyl)phenyl]borate **4b**,[10] *s*-$BuNH_3^+$ tetrakis[3,5-bis(trifluoromethyl)phenyl]borate **4c**,[10] *i*-$PrNH_3^+$ tetrakis[3,5-bis-(trifluoromethyl)phenyl]borate **4d**,[10] di-*n*-pentylammonium tetrakis-[3,5-bis(trifluoromethyl)phenyl]borate **5c**,[6a] and sodium tetrakis[3,5-bis(trifluoromethyl)phenyl]borate[8b] were synthesized according to literature procedures. NMR spectra were recorded on 250, 300, 400, or 500 MHz spectrometers; chemical shifts are reported relative to the residual solvent peak. The temperature was maintained at 298 K for all NMR spectra. COSY-45 spectra were taken using a relaxation delay of 2 s with 30 scans and 170 increments of 2048 points each. ROESY spectra were measured on a 400 MHz spectrometer with a mixing time t_m of 200 ms. Monte Carlo conformational searches (10000 steps) were performed with MacroModel-9.0/Maestro-4.1 program using $CHCl_3$ as solvent (GB/SA model).

7,13,19,25-Tetra-*tert*-butyl-27,28,29,30-tetrahexyloxy-2,3-dihomo-3-oxacalix[4]arene (3b). A mixture of 1.0 g (1.5 mmol) of *p-tert*-butyldihomooxacalix[4]arene and 0.72 g (18 mmol) of NaH (60% oil dispersion) in 56 mL of THF–DMF (7:1, v/v) was stirred under an atmosphere of N_2. After 2 h, 2.7 mL (18 mmol) of 1-iodohexane was added, and the mixture was stirred under reflux for 20 h. After cooling, the solvent was evaporated under reduced pressure, and the residue was dissolved in CH_2Cl_2 and washed with 1 M HCl (2 × 50 mL), NH_4Cl saturated solution (3 × 40 mL), and brine (50 mL). The organic layer was dried over Na_2SO_4 and filtered, and the solvent was removed under reduced pressure. The crude product was subjected to flash chromatography on silica gel (eluent gradient from CH_2Cl_2 to CH_2Cl_2/MeOH, 98:2), followed by recrystallization from MeOH, to give **3b** as a white solid (0.35 g, 23% yield): mp 101–102.5 °C; ESI(+) MS m/z = 1016 (MH^+); ^1H NMR ($CDCl_3$, 500 MHz, 298 K) δ 0.92 (t, CH_3, J = 6.8 Hz, 6H), 0.94 (t, CH_3, J = 6.8 Hz, 6H), 0.95, 1.18 [s, $C(CH_3)_3$, 18H each], 1.37 (m, $OCH_2CH_2CH_2$-$CH_2CH_2CH_3$, 20H,), 1.49 (m, $OCH_2CH_2CH_2CH_2CH_2CH_3$, 4H), 1.82, 1.94 (m, $OCH_2CH_2CH_2CH_2CH_2CH_3$, 4H each), 3.16 and 4.42 (AX, J = 13.4 Hz, $ArCH_2Ar$, 4H), 3.21 and 4.42 (AX, J = 12.9 Hz, $ArCH_2Ar$, 2H), 3.60, 3.66, 3.76, 3.82 (m, $OCH_2CH_2CH_2CH_2CH_2$-CH_3, 2H each), 4.61 and 4.67 (ABq, J = 13.6 Hz, CH_2OCH_2, 4H), 6.69, 6.95, 6.97, 7.05 (d, ArH, 2H each); ^{13}C NMR ($CDCl_3$, 125.8 MHz) δ 14.1, 14.2 [$O(CH_2)_5CH_3$], 22.8, 22.9 [$O(CH_2)_4CH_2CH_3$], 25.9, 26.1 [$O(CH_2)_2CH_2(CH_2)_2CH_3$], 30.1, 30.2 [$OCH_2CH_2(CH_2)_3CH_3$], 30.6, 30.7 ($ArCH_2Ar$), 31.5 ($C(CH_3)_3$), 32.1, 32.2 [$O(CH_2)_3CH_2CH_2CH_3$], 34.0 ($C(CH_3)_3$), 68.0 ($CH_2OCH_2$), 74.4, 75.0 [$OCH_2(CH_2)_4CH_3$], 123.3, 125.5, 125.6

dx.doi.org/10.1021/jo3019945 | J. Org. Chem. 2012, 77, 10285–10293

(ArH), 131.2, 133.4, 134.1, 144.5, 144.9, 152.4, 153.3 (Ar). Anal. Calcd for $C_{69}H_{106}O_5$: C, 81.60; H, 10.52. Found: C, 81.69; H, 10.46.

General Procedure for the Synthesis of Diethylammonium 5a and Di-*n*-propylammonium 5b Tetrakis[3,5-bis(trifluoromethyl)phenyl]borate (TFPB) Salts. A solution of sodium tetrakis[3,5-bis(trifluoromethyl)phenyl]borate[8b] (0.67 mmol) in dry methanol (2 mL) was added to the solution of appropriate dialkylammonium chloride salts (diethylammoinum chloride or di-*n*-propylammonium chloride, 0.52 mmol) in dry methanol (3 mL). The resulting solution was stirred overnight. After methanol was removed by evaporation, deionized water was added, and the brown solid was filtered off and dried under vacuum for 24−48 h. **5a·TFPB⁻**: mp 156.2−156.7 °C; ESI(+) MS m/z = 75 (M − TFPB⁻)⁺; ^{1}H NMR (CD_3OD, 250 MHz, 298 K) δ 1.29 [t, $(CH_3CH_2)_2NH_2^+$, J = 7.2 Hz, 6H], 3.03 [q, $(CH_3CH_2)_2NH_2^+$, J = 7.2 Hz, 4H], 7.60 (br s, ArH^{TFPB}, 12 H). Anal. Calcd for $C_{36}H_{24}BF_{24}N$: C, 46.13; H, 2.58; N, 1.49. Found: C, 46.23; H, 2.49; N, 1.60.

5b·TFPB⁻: mp 157.6−158.0; ESI(+) MS m/z = 103 (M−TFPB⁻)⁺; ^{1}H NMR (CD_3OD, 400 MHz, 298 K) δ 0.97 [t, $(CH_3CH_2CH_2)_2NH_2^+$, J = 7.6 Hz, 6H], 1.66 [m, $(CH_3CH_2CH_2)_2NH_2^+$, 4H], 2.90 [t, $(CH_3CH_2CH_2)_2NH_2^+$, J = 7.6 Hz, 4H], 7.60 (br s, ArH^{TFPB}, 12 H). Anal. Calcd for $C_{38}H_{28}BF_{24}N$: C, 47.28; H, 2.92; N, 1.45. Found: C, 47.38; H, 2.83; N, 1.54.

General Procedure for the Preparation of Alkylammonium Complexes of 3a. Dihomooxacalix[4]arene derivative **3a** (1.23×10^{-3} mmol) and the appropriate alkylammonium TFPB salt **4a−d** (1.23×10^{-3} mmol) were dissolved in $CDCl_3$ (0.4 mL, 3.0×10^{-3} M solution). The solution was sonicated for 15 min at room temperature and transferred to an NMR tube for 1D and 2D NMR spectra acquisition.

Determination of K_{assoc} Values of *t*-BuNH$_3^+$⊂3a, *s*-BuNH$_3^+$⊂3a, and *i*-PrNH$_3^+$⊂3a Complexes by Quantitative ^{1}H NMR Analysis.[17b] The samples were prepared by dissolving **3a** (1.24×10^{-3} mmol) and the appropriate alkylammonium guest **4b**, **4c**, or **4d** (1.24×10^{-3} mmol) in $CDCl_3$ (0.4 mL) containing 1 μL of 1,1,2,2-tetrachloroethane (d = 1.59 g/mL) as internal standard. The complex concentration [complex] was evaluated by integration of the ^{1}H NMR signal of $CHCl_2CHCl_2$ vs the shielded signals at negative values of the guest molecule. The following equation[17b] was used to obtain the moles of the complex:

$$\frac{G_a}{G_b} = \frac{F_a}{F_b} \times \frac{N_a}{N_b} \times \frac{M_a}{M_b}$$

where

G_a = grams of 1,1,2,2-tetrachloroethane; G_b = grams of complex

F_a and F_b = areas of the signals of 1,1,2,2-tetrachloroethane and shielded signal of the guest

N_a and N_b = numbers of nuclei which cause the signals (N_a for 1,1,2,2-tetrachloroethane; N_b for guest)

M_a and M_b = molecular masses of 1,1,2,2-tetrachloroethane (a) and complex (b)

Determination of K_{assoc} Values of *n*-BuNH$_3^+$⊂3a Complex by Competition ^{1}H NMR Experiment. A ^{1}H NMR competition experiment was performed by analysis of a 1:1:1 mixture of host H, guest GA, and guest GB in a NMR tube using $CDCl_3$ as solvent. In a typical experiment, 0.4 mL of solution of Host, 3.0×10^{-3} M in $CDCl_3$, were mixed with 0.012 mL of 0.1 M solution of guest GA and 0.012 mL of 0.1 M solution of guest GB. The following equations[17b] were used:

$$K_{A\subset H} = \frac{[HG_A]}{[H][G_A]} \text{ and } K_{B\subset H} = \frac{[HG_B]}{[H][G_B]}$$

$$\downarrow$$

$$K_{rel} = \frac{K_{A\subset H}}{K_{B\subset H}} = \frac{[HG_A][H][G_B]}{[HG_B][H][G_A]} \rightarrow \begin{matrix}[HG_A] = [G_B] \\ [HG_B] = [G_A]\end{matrix}$$

$$\text{then } K_{rel} = \frac{K_{A\subset H}}{K_{B\subset H}} = \frac{[HG_A]^2}{[HG_B]^2}$$

The complex concentrations $[HG_A]$ and $[HG_B]$ were evaluated by integration of the corresponding ^{1}H NMR signals.

Determination of Association Constants of 5a⊂3a, 5a⊂3b, 5b⊂3b, and 5c⊂3b Complexes by ^{1}H NMR Titrations.[17a] ^{1}H NMR titrations were performed at 298 K in $CDCl_3$. The host concentration was kept constant while the guest concentration was varied, for example: **3a**, 5 mM and di-*n*-ethylammonium·TFPB⁻ **5a**, 0.5−10 mM; **3b**, 5 mM and di-*n*-ethylammonium·TFPB⁻ **5a**, 0.5−10 mM; **3b**, 5 mM and di-*n*-propylammonium·TFPB⁻ **5b**, 0.5−10 mM; **3b**, 5 mM and di-*n*-pentylammonium·TFPB⁻ **5c**, 0.5−10 mM. In all cases, the signals of the host were followed and the data were analyzed by a nonlinear regression analysis.[17a]

Job Plot Experiments.[17a] Complexation stoichiometry was determined by a Job plot using ^{1}H NMR spectroscopy.[17a] Stock solutions of host (5 mM) and guest (5 mM) in $CDCl_3$ were prepared. Ten NMR spectra were obtained in the following volume ratios (host/guest): 100:400, 150:350, 200:300, 250:250, 300:200, 350:150, 400:100, 450:50, 500:0 (μL/μL). The chemical shift of methylene protons were recorded for each sample, the corresponding concentration of complex was determined for each sample, and the Job plot was obtained by plotting complex concentration as a function of the mole fraction of the host.[17a]

■ ASSOCIATED CONTENT

Ⓢ Supporting Information

^{1}H NMR spectra of new compounds **3b**, **5a**, and **5b** and 2D COSY and ROESY spectra. This material is available free of charge via the Internet at http://pubs.acs.org.

■ AUTHOR INFORMATION

Corresponding Author

*E-mail: cgaeta@unisa.it; neri@unisa.it; pmmarcos@fc.ul.pt.

Notes

The authors declare no competing financial interest.

■ ACKNOWLEDGMENTS

Thanks are due to Dr. Patrizia Iannece (Dipartimento di Chimica, Università di Salerno) for ESI-MS measurements.

■ REFERENCES

(1) For comprehensive reviews on calixarene macrocycles, see: (a) Gutsche, C. D. *Calixarenes, An Introduction*; Royal Society of Chemistry: Cambridge, UK, 2008, Chapter 5, pp 116−128. (b) Böhmer, V. *Angew. Chem., Int. Ed. Engl.* **1995**, *34*, 713−745. (c) Gutsche, C. D. *Calixarenes Revisited*; Royal Society of Chemistry: Cambridge, 1998. (d) *Calixarenes 2001*; Asfari, Z., Böhmer, V., Harrowfield, J., Vicens, J., Eds.; Kluwer: Dordrecht, 2001. (e) Böhmer, V. In *The Chemistry of Phenols*; Rappoport, Z., Ed.; Wiley: Chichester, UK, 2003; Chapter 19. (f) *Calixarenes in the Nanoworld*; Vicens, J., Harrowfield, J., Eds.; Springer, Dordrecht, 2007.

(2) Special issue on cyclodextrins: *Chem. Rev.* **1998**, *98*, 1741−2076.

(3) Gokel, G. W. *Crown Ethers and Cryptands: Monographs in Supramolecular Chemistry*; The Royal Society of Chemistry: Cambridge, 1991.

(4) Lagona, J.; Mukhopadhyay, P.; Chakrabarti, S.; Isaacs, L. *Angew. Chem., Int. Ed.* **2005**, *44*, 4844−4870.

(5) (a) Masci, B.; Levi Mortera, S.; Persiani, D.; Thuéry, P. *J. Org. Chem.* **2006**, *71*, 504−511. (b) Masci, B. In *Calixarenes 2001*; Asfari, Z., Böhmer, V., Harrowfield, J., Vicens, J., Eds.; Kluwer: Dordrecht, 2001; pp 235−249. (c) Masci, B.; Finelli, M.; Varrone, M. *Chem.—Eur. J.* **1998**, *4*, 2018−2030. (d) Marcos, P. M.; Ascenso, J. R.; Lamartine, R.; Pereira, J. L. C. *Tetrahedron* **1997**, *53*, 11791−11802.

(6) (a) Gaeta, C.; Troisi, F.; Neri, P. *Org. Lett.* **2010**, *12*, 2092−2095. (b) Talotta, C.; Gaeta, C.; Pierro, T.; Neri, P. *Org. Lett.* **2011**, *13*, 2098−2101. (c) Pierro, T.; Gaeta, C.; Talotta, C.; Casapullo, A.; Neri, P. *Org. Lett.* **2011**, *13*, 2650−2653. (d) Talotta, C.; Gaeta, C.; Neri, P. *Org. Lett.* **2012**, *14*, 3104−3107.

(7) For a review on the recognition abilities of calixarene macrocycles toward organic cations, see: Abraham, W. *J. Inclusion Phenom. Macrocycl. Chem.* **2002**, *43*, 159−174. For recent reports, see: (a) Gattuso, G.; Notti, A.; Pappalardo, S.; Parisi, M. F.; Pilati, T.; Terraneo, G. *CrystEngComm* **2012**, *14*, 2621−2625. (b) Capici, C.; Cohen, Y.; D'Urso, A.; Gattuso, G.; Notti, A.; Pappalardo, A.; Pappalardo, S.; Parisi, M. F.; Purrello, R.; Slovak, S.; Villari, V. *Angew. Chem., Int. Ed.* **2011**, *50*, 11956−11961. (c) Le Gac, S.; Picron, J.-F.; Reinaud, O.; Jabin, J. *Org. Biomol. Chem.* **2011**, *9*, 2387−2396. (d) Monnereau, C.; Rebilly, J.-N.; Reinaud, O. *Eur. J. Org. Chem.* **2011**, 166−175. (e) Moerkerke, S.; Ménand, M.; Jabin, I. *Chem.—Eur. J.* **2010**, *16*, 11712−11719. (f) Capici, C.; De Zorzi, R.; Gargiulli, C.; Gattuso, G.; Geremia, S.; Notti, A.; Pappalardo, S.; Parisi, M. F.; Puntoriero, F. *Tetrahedron* **2010**, *66*, 4987−4993. (g) Gargiulli, C.; Gattuso, G.; Liotta, C.; Notti, A.; Parisi, M. F.; Pisagatti, I.; Pappalardo, S. *J. Org. Chem.* **2009**, *74*, 4350−4353. (h) Ménand, M.; Jabin, I. *Org. Lett.* **2009**, *11*, 673−676. (i) Coquière, D.; de la Lande, A.; Martì, S.; Parisel, O.; Prangé, T.; Reinaud, O. *Proc. Natl. Acad. Sci. U.S.A.* **2009**, *106*, 10449−10454 and references therein. (j) Le Gac, S.; Ménand, M.; Jabin, I. *Org. Lett.* **2008**, *10*, 5195−5198. (k) Hamon, M.; Ménand, M.; Le Gac, S.; Luhmer, M.; Dalla, V.; Jabin, I. *J. Org. Chem.* **2008**, *73*, 7067−7071. (l) Gattuso, G.; Notti, A.; Pappalardo, A.; Parisi, M. F.; Pisagatti, I.; Pappalardo, S.; Garozzo, D.; Messina, A.; Cohen, Y.; Slovak, S. *J. Org. Chem.* **2008**, *73*, 7280−7289.

(8) (a) Strauss, S. H. *Chem. Rev.* **1993**, *93*, 927−942. (b) Nishida, H.; Takada, N.; Yoshimura, M.; Sonoda, T.; Kobayashi, H. *Bull. Chem. Soc. Jpn.* **1984**, *57*, 2600−2604. For recent examples on the use of TFPB superweak anion in supramolecular chemistry, see: (c) Li, C.; Shu, X.; Li, J.; Fan, J.; Chen, Z.; Weng, L.; Jia, X. *Org. Lett.* **2012**, *14*, 4126−4129. (d) Blight, B. A.; Camara-Campos, A.; Djurdjevic, S.; Kaller, M.; Leigh, D. A.; McMillan, F. M.; McNab, H.; Slawin, A. M. *J. Am. Chem. Soc.* **2009**, *131*, 14116−14122. (e) Hou, H.; Leung, K. C.-F.; Lanari, D.; Nelson, A.; Stoddart, J. F.; Grubbs, R. H. *J. Am. Chem. Soc.* **2006**, *128*, 13358−13359. For a review on counterion effects in supramolecular chemistry, see: (f) Gasa, T. B.; Valente, C.; Stoddart, J. F. *Chem. Soc. Rev.* **2011**, *40*, 57−78.

(9) For a review on the chemistry of calix[7]arenes, see: Martino, M.; Neri, P. *Mini-Rev. Org. Chem.* **2004**, *1*, 219−231. For reports on the functionalization of calix[7]arene macrocycle, see: (a) Li, H.; Xiong, D.; Chen, Y.; Xie, P.; Wan, J. *J. Incl. Phenom. Macrocycl. Chem.* **2008**, *60*, 169−172. (b) Luo, Z. Y.; Gong, S. L.; Zhang, C. L.; Zheng, Q.; Chen, Y. Y. *Synlett* **2006**, *5*, 795−797. (c) Martino, M.; Gaeta, C.; Neri, P. *Tetrahedron. Lett.* **2004**, *45*, 3387−3391. (d) Martino, M.; Gaeta, C.; Gregoli, L.; Neri, P. *Tetrahedron. Lett.* **2002**, *43*, 9521−9525. (e) Martino, M.; Gregoli, L.; Gaeta, C.; Neri, P. *Org. Lett.* **2002**, *4*, 1531−1534.

(10) Gaeta, C.; Talotta, C.; Farina, F.; Camalli, M.; Campi, G.; Neri, P. *Chem.—Eur. J.* **2012**, *18*, 1219−1230.

(11) Chen, N.-C.; Chuang, C.-J.; Wang, L.-Y.; Lai, C.-C.; Chiu, S.-H. *Chem.—Eur. J.* **2012**, *18*, 1896−1890.

(12) (a) Pappalardo, S.; Parisi, M. F. *J. Org. Chem.* **1996**, *61*, 8724−8725. (b) Arnaud-Neu, F.; Fuangswasdi, S.; Notti, A.; Pappalardo, S.; Parisi, M. F. *Angew. Chem., Int. Ed.* **1998**, *37*, 112−114. (c) De Salvo, G.; Gattuso, G.; Notti, A.; Parisi, M. F.; Pappalardo, S. *J. Org. Chem.* **2002**, *67*, 684−692. (d) Cafeo, G.; Gattuso, G.; Kohnke, F. H.; Notti, A.; Occhipinti, S.; Pappalardo, S.; Parisi, M. F. *Angew. Chem., Int. Ed.* **2002**, *41*, 2122−2126.

(13) Recently, an example of threading through the conformationally blocked pentakis(*tert*-butoxycarbonylmethoxy)-*p*-*tert*-butylcalix[5]arene derivative has been reported: Gattuso, G.; Notti, A.; Parisi, M. F.; Pisagatti, I.; Amato, M. E.; Pappalardo, A.; Pappalardo, S. *Chem.—Eur. J.* **2010**, *16*, 2381−2385.

(14) This point has also been addressed for crown ether macrocycles: (a) Zhang, C.; Li, S.; Zhang, J.; Zhu, K.; Li, N.; Huang, F. *Org. Lett.* **2007**, *9*, 5553−5556. (b) Hsu, C.-C.; Chen, N.-C.; Lai, C.-C.; Liu, Y.-H.; Peng, S.-M.; Chiu, S.-H. *Angew. Chem., Int. Ed.* **2008**, *47*, 7475−7478.

(15) See the Supporting Information for further details.

(16) Molecular modeling was performed with MacroModel-9.0/Maestro-4.1 program: Mohamadi, F.; Richards, N. G.; Guida, W. C.; Liskamp, R.; Lipton, M.; Caufield, C.; Chang, G.; Hendrickson, T.; Still, W. C. *J. Comput. Chem.* **1990**, *11*, 440−467.

(17) (a) Hirose, K. In *Analytical Methods in Supramolecular Chemistry*; Schalley, C. A., Eds.; Wiley-VCH: Weinheim, 2007; Chapter 2, pp 17−54. (b) *150 and More Basic NMR Experiments: A Practical Course*; Braun, S., Kalinowsky, H.-O., Berger, S., Eds.; Wiley-VCH: Weinheim, 1996; pp 232 −233.

(18) Pappalardo and co-workers have previously reported that the presence of *tert*-butyl substituents at the upper rim of 20-membered-ring calix[5]arene hosts sterically interfere with the penetration of branched alkylammonium guests, into calix[5]arene cavities, see ref 12a,c.

(19) For recent reports on the transfer of chirality between chiral guest to achiral host detected by CD spectroscopy, see: (a) Petrovic, A. G.; Vantomme, G.; Negron-Abril, Y. L.; Lubian, E.; Saielli, G.; Menegazzo, I.; Cordero, R.; Proni, G.; Nakanishi, K.; Carofiglio, T.; Berova, N. *Chirality* **2011**, *23*, 808−819. (b) Berova, N.; Pecitelli, G.; Petrovic, A. G.; Proni, G. *Chem. Commun.* **2009**, 5958−5980. (c) Shundo, A.; Labuta, J.; Hill, J. P.; Ishihara, S.; Ariga, K. *J. Am. Chem. Soc.* **2009**, *131*, 9494−9495. (d) Katoono, R.; Kawai, H.; Fujiwara, K.; Suzuki, T. *J. Am. Chem. Soc.* **2009**, *131*, 16896−16904.

(20) In fact, has been seen that long *n*-alkanes, such as *n*-tetradecane, are coiled to adopt helical conformations within Rebek's self-assembled capsule. The generated unfavorable gauche interactions are compensated by the favorable CH/π interactions with the fixed aromatic walls of the host; see: (a) Scarso, A.; Trembleu, L.; Rebek, J., Jr. *Angew. Chem., Int. Ed. Engl.* **2003**, *42*, 5499−5502. Scarso, A.; Trembleu, L.; Rebek, J., Jr. *J. Am. Chem. Soc.* **2004**, *126*, 13512−13518.